Polymers **2015**, *7*, 266-280; doi:10.3390/polym7020266

OPEN ACCESS

polymers

ISSN 2073-4360

www.mdpi.com/journal/polymers

Article

P(MMA-EMA) Random Copolymer Electrolytes Incorporating Sodium Iodide for Potential Application in a Dye-Sensitized Solar Cell

Nurul Akmaliah Dzulkurnain [1], Azizan Ahmad [2] and Nor Sabirin Mohamed [3,*]

[1] Institute of Graduate Studies, University of Malaya, 50603 Kuala Lumpur, Malaysia; E-Mail: nurulakmaliah86@gmail.com

[2] School of Chemistry Science and Food Technology, Faculty of Science and Technology, Universiti Kebangsaan Malaysia, 43600 Bangi, Selangor Darul Ehsan, Malaysia; E-Mail: azizan@ukm.my

[3] Centre for Foundation Studies in Science, University of Malaya, 50603 Kuala Lumpur, Malaysia

* Author to whom correspondence should be addressed; E-Mail: nsabirin@um.edu.my; Tel.: +603-7967-5972.

Academic Editor: Thomas Junkers

Received: 19 December 2014 / Accepted: 1 February 2015 / Published: 9 February 2015

Abstract: Polymer electrolytes based on 90 wt% of methyl methacrylate and 10 wt% of ethyl methacrylate (90MMA-co-10EMA) incorporating different weight ratios of sodium iodide were prepared using the solution casting method. The complexation between salt and copolymer host has been investigated using Fourier transform infrared spectroscopy. The ionic conductivity and thermal stability of the electrolytes were measured using impedance spectroscopy and differential scanning calorimetry, respectively. Scanning electron microscopy was used to study the morphology of the polymer electrolytes. The ionic conductivity and glass transition temperature increased up to 20 wt% of sodium iodide (5.19×10^{-6} S·cm^{-1}) and decreased with the further addition of salt concentration, because of the crosslinked effect. The morphology behavior of the highest conducting sample also showed smaller pores compared to the other concentration. The total ionic transference number proved that this system was mainly due to ions, and the electrochemical stability window was up to 2.5 V, which is suitable for a dye-sensitized solar cell application. This sample was then tested in a dye-sensitized solar cell and exhibited an efficiency of 0.62%.

Keywords: ionic conductivity; polymer electrolyte; transference number; electrochemical stability; dye-sensitized solar cell

1. Introduction

Dye-sensitized solar cells (DSSCs) have received considerable attention since the pioneering work of O' Regan and Grätzel [1], due to the high conversion efficiency, low manufacturing cost and simple preparation technique. However, most of the cells that give high efficiency utilize liquid electrolytes, which cause some problems, such as leakage and volatilization, corrosion at the counter electrode, difficulty in fabrication and limited long-term performance [2]. Thus, replacing liquid electrolytes with solid polymer electrolytes (SPEs) has become one of the approaches to overcome these problems. Besides, SPEs have been reported to show promising results for application in DSSCs [2,3]. SPEs are also safer, free from leakage problems, show good thermal stability and are easier to handle for device fabrication [4–6].

Generally, SPEs exhibit low ionic conductivity at room temperature [7,8]. Therefore, attempts should be made to improve the ionic conductivity, which, in turn, will improve the device performance, such as modifying the polymer host using the photo-polymerization technique. Based on Bella *et al.*, this technique is a solvent-free technique that encourages the formation of polymer networks with tailored physical-chemical, functional and mechanical properties through the rapid transformation of the liquid monomer into a solid membrane. It was carried out at room temperature under UV light in a few minutes; therefore, it guarantees time and energy savings [9–11]. In our previous work, the modification of the polymer host was done by copolymerizing two types of methacrylate monomers, which were methyl methacrylate (MMA) and ethyl methacrylate (EMA), with different weight ratios. The copolymer with a MMA:EMA weight ratio of 90:10 showed the lowest glass transition temperature (T_g), the greatest amorphous region and low bulk resistivity [12]. Therefore, for the present study, this copolymer was utilized to obtain polymer electrolytes for a possible application in a DSSC.

Previously, Imperiyka *et al.* reported the study of glycidyl methacrylate-*co*-methyl methacrylate (GMA-*co*-MMA) copolymer electrolytes using $LiClO_4$ and $LiCF_3SO_3$ as the doping salts for application in lithium ion batteries [13,14]. However, there are concerns about the cost of lithium if the demands for this technology stretch into larger scale transport and electrochemical device applications. Therefore, to overcome this problem, sodium-based electrolytes have been selected for the present study. The selection of the salt is due to its lower cost, ready availability, lower toxicity and low atomic mass [15–17]. Besides that, a comparative study on the effect of sodium and lithium triflate in polyacrylonitrile (PAN), which was reported by Osman *et al.* found that the sodium-based electrolyte system possessed higher ionic conductivity at room temperature [18]. In addition, in terms of the DSSC application, salts with a halide anion should be used in order to provide redox coupling in the DSSCs.

For this work, solid polymer electrolyte films were prepared by adding sodium iodide (NaI) in the 90MMA-*co*-10EMA polymer host, and then the effect of NaI salt concentration on the ionic conductivity, the thermal behavior and the cross-sectional morphology were investigated. The ionic transference number and electrochemical stability windows of the highest conducting sample were then investigated before it was used for DSSC fabrication.

2. Experimental Section

2.1. Materials

MMA contains ≤ 30 ppm Mono Methyl Ether Hydroquinone (MEHQ) as the inhibitor, 99% (M_w = 100.12 g/mol, Sigma Aldrich, St. Louis, MI, USA). EMA contains 15–20 ppm monomethyl ether hydroquinone as the inhibitor, 99% (M_w = 114.14 g/mol, Sigma Aldrich). 2,2-dimethoxy-2-phenylacetophenone, 99% (DMPA, M_w = 256.30 g/mol, Sigma Aldrich), sodium iodide American Chemical Society (ACS) reagent, ≥99.5% (NaI, M_w = 149.89 g/mol, Sigma Aldrich), methanol (M_w = 32.04 g/mol, System® ChemAR®, Kielce, Poland), iodine (Merck, Darmstadt, Germany) and tetrahydrofuran (THF, M_w = 72.11 g/mol, R&M Chemicals, Edmonton, Canada) were the chemicals used for polymer electrolyte preparation in this study. For the DSSC components, cis-diisothiocyanato-bis(2,2'-bipyridyl-4,4'-dicarboxylato) ruthenium(II) bis(tetrabutylammonium) dye (N-719), platinum paste, under the commercial name Platisol T, and fluorine-doped tin oxide (FTO) with ~15 $\Omega \cdot cm^{-2}$ as the transparent conductive oxide were purchased from Solaronix (Aubonne, Switzerland). Titanium dioxide (TiO_2) paste (DSL 18NR-AO Active Opaque Titania Paste) was supplied by DyeSol (New South Wales, Australia). All materials were used without purification.

2.2. Synthesis of Polymer

90 wt% MMA and 10 wt% of EMA were copolymerized in the presence of a photo-initiator, DMPA, by using a ratio of 1:0.016. The mixture was stirred until the DMPA completely dissolved and was exposed to a UV radiation box with four 15-W UV lamps in a nitrogen environment for 5 min. This preparation technique was reported in the authors' earlier paper [12]. The copolymer was then washed with methanol to remove residual monomers.

2.3. Preparation of Solid Polymer Electrolytes

Three grams of 90MMA-*co*-10EMA copolymer were added with several weight percentages of NaI, which were 10 wt%, 20 wt%, 30 wt% and 40 wt%, in separate beakers. The mixtures of the copolymer and sodium salt were dissolved in 30 mL THF and stirred using magnetic stirrers for 24 h at 40 °C. The homogenous solutions of the electrolytes were then poured into glass petri dishes and dried in a vacuum oven at 40 °C for 4 h. The free standing films were peeled off from the glass petri dishes before being subjected to characterizations.

2.4. Characterization

Fourier transform infrared (FTIR) was used to identify the interaction between polymer hosts with doping salt. The analysis was done at room temperature using a Perkin Elmer (Waltham, MA, USA) Frontier FTIR spectrophotometer in the range of 4000 to 550 cm^{-1} with a scanning resolution of 2 cm^{-1}.

Impedance measurements of the samples were performed using a SOLARTRON 1260 impedance analyzer over the frequency range from 10 Hz to 5 MHz with a 100-mV DC amplitude. The samples were sandwiched between stainless steel electrodes at room temperature, and the room temperature ionic conductivity value was calculated using the following equation:

$$\sigma = \frac{t}{R_b A} \quad (1)$$

where t is the sample thickness, A is the sample-electrode contact area and R_b is the bulk resistance obtained from the plots of the real impedance, Z', against the imaginary impedance, Z''. The mathematical equation of impedance can be written as:

$$Z^* = Z' + iZ'' \quad (2)$$

The samples were further analyzed for a temperature dependence study in the temperature range of 300 to 328 K to study the effect of temperature on the ionic conductivity. The temperature was controlled using ESPEC SU-242, a temperature chamber (Hudsonville, MI, USA) which was connected to the SOLARTRON 1260 impedance/gain phase analyzer (Kingston on Thames, UK).

Differential scanning calorimetry (DSC) measurements were carried out on the prepared samples to provide information about the phase transition temperatures. Approximately 5–6 mg of prepared polymer electrolyte sample were tested over a temperature range of 30–250 °C at a scanning rate of 10 °C·min^{-1} using a DSC 131 EVO (SETARAM Instruments, Caluire, France). The data were evaluated using Calisto processing software to determine the glass transition temperature from the onset of the heat capacity change on the heating ramp.

The cross-sectional morphology of the polymer electrolyte films was observed using a Zeiss (Oberkochen, Germany) EVO MA10 scanning electron microscope at 500× magnification with an accelerating voltage of 10.0 kV. The samples were prepared by breaking them into small rectangular shapes and were coated with gold under vacuum condition.

The total ionic transference numbers (t_{ion}) for the films were determined based on the analysis of the dc polarization technique on the symmetrical cell with stainless steel as the blocking electrodes. This is used to discriminate between electronic and ionic conduction in polymer electrolytes. From the normalized polarization current *versus* time plots, the total number of ions transported in these polymer electrolytes can be calculated using the equation:

$$t_{ion} = 1 - I_{ss} \quad (3)$$

where I_{ss} is the steady-state current.

The electrochemical stability window of the highest conducting sample was obtained using linear sweep voltammetry (LSV), which was done on a Wonatech ZIVE MP2 Multichannel electrochemical workstation (Seoul, Korea). The LSV measurement was carried out in the range from 0 to 5 V at a scanning rate of 100 mV·s^{-1}, with stainless steel as the blocking electrodes at room temperature.

2.5. Photoelectrochemical Cell Fabrication and Characterization

Photoanode glass was spread with TiO_2 paste using the doctor blade technique with the support of adhesive tape to prevent it from moving. Then, the TiO_2 photoanode electrode was annealed at 450 °C for 30 min in order to change the anatase phase into the rutile phase and was immersed in 0.3 mM of N-719 dye solution at room temperature for 24 h. Besides that, a platinized FTO counter electrode was prepared by the brushing-painting technique and annealed at 450 °C for 30 min to activate the quasi-transparent platinum layer. The P(MMA-*co*-EMA)-NaI solution that gave higher conductivity was added with iodine (I_2) at a molar ratio of 10:1, cast onto the TiO_2 photoanode electrodes and left to dry

at room temperature. The current-voltage (*I–V*) data of the FTO/TiO_2-dye/P(MMA-*co*-EMA)-NaI/I_2/Pt DSSC were recorded by Zive Smart Manager software version 5.0.0.5, with a xenon light source, at room temperature (dark atmosphere) and under AM (air mass) 1.5 illumination at a light intensity of 100 mW·cm^{-2}, controlled by a radiometer. The illumination cell area was set to 1 cm^2. The photoelectric performances, such as the fill factor, FF and light-to-electricity energy conversion efficiency, η, were calculated using Equations (4) and (5), respectively:

$$\mathrm{FF} = \frac{V_{\max} \times J_{\max}}{V_{OC} \times J_{sc}} \tag{4}$$

$$\eta = \frac{V_{OC} \times J_{SC} \times \mathrm{FF} \times 100}{P_{\mathrm{in}}} \tag{5}$$

where V_{OC} is the open circuit voltage (V), J_{SC} is the short circuit current density (mA·cm^{-2}), P_{in} is the incident light power density (mW·cm^{-2}), while V_{max} (V) and J_{max} (mA·cm^{-2}) are the voltage and the current density in the *J–V* curves, respectively, at the point of maximum power output [19].

3. Results and Discussion

3.1. FTIR Analysis

FTIR spectroscopy was used to study the vibration energy of covalent bonds in the polymer host due to the interactions that occurred when salt was introduced into the polymer [20]. Figure 1 shows the FTIR spectra at the selected regions of interest. The main regions of interest are for oxygen atoms of the carbonyl group (C=O) located around the wavenumber of 1750–1730 cm^{-1}, for ether group (C–O–C) at 1300–1000 cm^{-1} and for the methyl group (CH_3) at 1440–1245 cm^{-1} from the MMA and EMA structure in P(MMA-*co*-EMA). This is because the oxygen atoms from these functional groups can act as electron donor atoms and form a coordinate or dative bond with sodium ions from the doping salts, hence forming a polymer-salt electrolyte [21,22]. Therefore, in these polymer electrolytes systems, the sodium iodide is assumed to be fully dissociated into cations and anions, then coordinated with the polymer host structure. The possible reaction mechanism between polymer host with the doping salt is shown in Figure 2. Figure 1 presents the FTIR spectra of the symmetrical stretching of the carbonyl group, ν(C=O), from the polymer host structure for various concentration of salts. With the addition of 10 wt%, 20 wt%, 30 wt% and 40 wt% of sodium salts, the peak was shifted from 1725 to 1719 cm^{-1}. The specific vibration mode of ether group (C–O–C) can also be observed in the spectra, which shows the –CH_3 asymmetric deformation of P(MMA-*co*-EMA) from σ(O–CH_3), the symmetric and asymmetric stretching mode of C–O–C and the asymmetrical stretching mode, ν_{as}(C–O–C), of the ether group at 1447, 1271, 1240 and 1144 cm^{-1}, respectively. With the addition of salts, these peaks shifted to the lower wavenumbers, which were 1444, 1267, 1236 and 1141 cm^{-1}. CH_3 asymmetric bending at 1434 cm^{-1} was shifted to 1431 cm^{-1}, and the CH_3 symmetric bending at 1239 cm^{-1} was shifted to 1236 cm^{-1}. All of the wavenumbers were shifted more than 2 cm^{-1}; therefore, this result is significant to prove the occurrence of complexation between the polymer host and the doping salt.

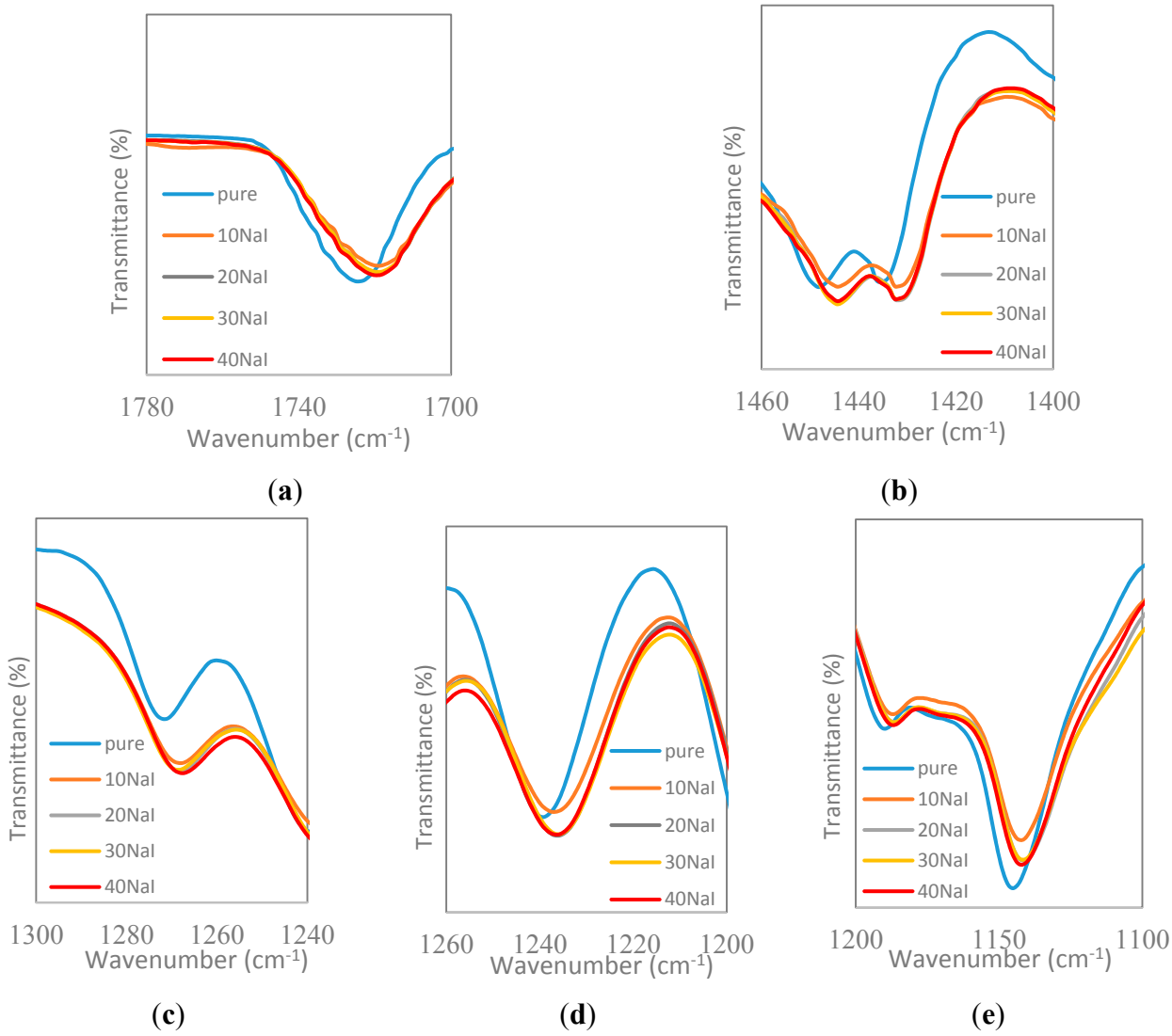

Figure 1. (**a**–**e**) FTIR spectra of the carbonyl, ether and methyl group of P(MMA-*co*-EMA) (MMA, methyl methacrylate; EMA, ethyl methacrylate) with the weight percentage ratios of NaI.

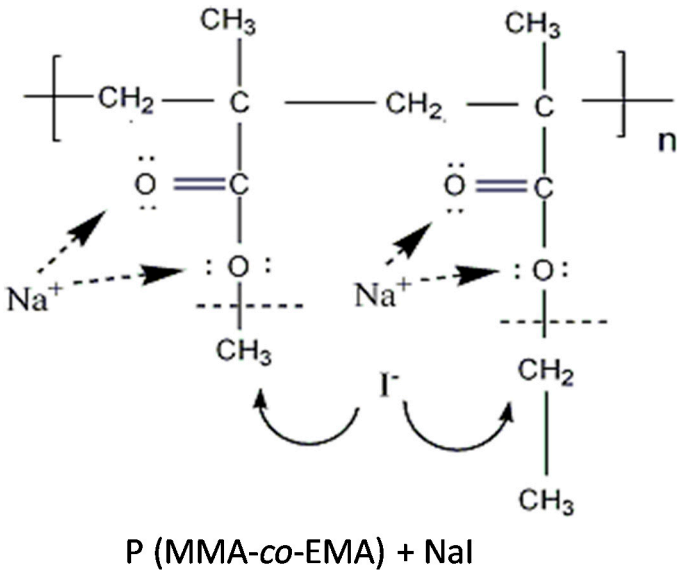

Figure 2. Possible mechanism of P(MMA-*co*-EMA) + NaI polymer electrolytes.

3.2. Conductivity and Thermal Analysis

Figure 3 shows the ionic conductivity and glass transition temperature (T_g) of copolymer electrolytes as a function of sodium salt concentration. The ionic conductivity increases with the increase of the concentration of salt until it reaches the optimum value of 5.19×10^{-6} S·cm^{-1} at 20 wt% of salt. The full dissociation of Na^+ and I^- in the polymer host structure shown in the FTIR analysis is a factor for the enhancement of the ionic conductivity. Therefore, the increase of salt content increases the number of mobile ions in the polymer matrix, resulting in the increase of ionic conductivity [23]. With the further increment of the salt concentration (up to 40 wt%), the ionic conductivity started to decrease. The decreases may be due to the excess dissociation of Na^+ and I^- attributed to the increase of the association rate of the ion, thus leading to the formation of ion clusters. This reduced the number of mobile charge carriers and the mobility of the ions, hence decreasing the ionic conductivity [14,24–26]. The content of salt was limited to 40 wt%, since the addition of salt of more than 40 wt% produced sticky films that were difficult to handle. The trend of T_g *versus* sodium salt concentration contradicts that of the ionic conductivity, because, generally, the conductivity is expected to decrease when the T_g increases [27,28]. According to Subban, this can be explained in terms of crosslinking that formed between the P(MMA-*co*-EMA) chain and sodium salts. In the polymer electrolyte system, the crosslinks are well separated in space and can move with respect to each other to a certain extent, thereby contributing to an increase in ionic conductivity [29]. Besides that, the anions that interact with the polymer may also contribute to the ionic conductivity, as mentioned earlier [30].

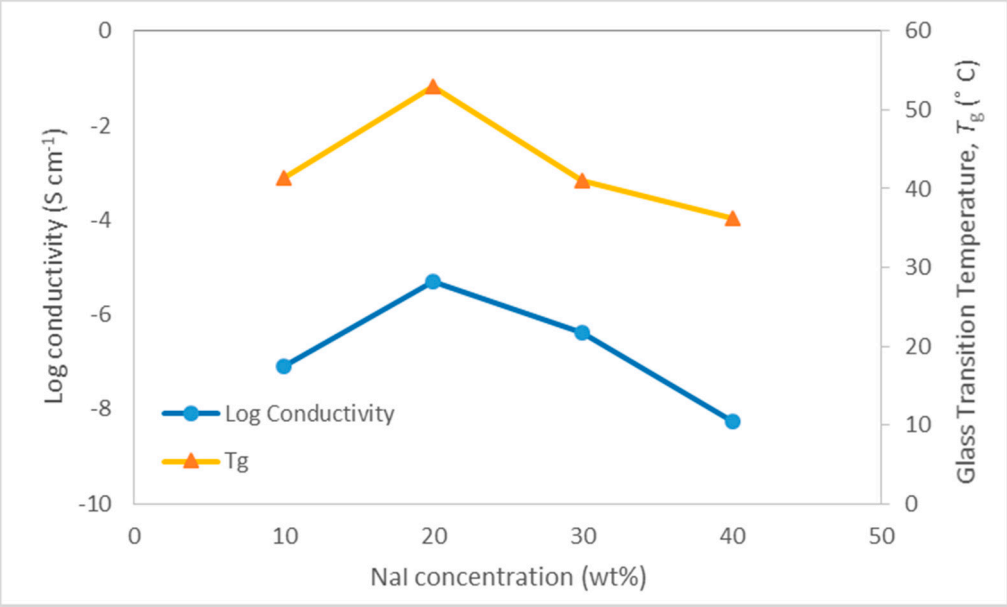

Figure 3. Log conductivity with the glass transition temperature (T_g) of P(MMA-*co*-EMA) with various concentrations of NaI.

3.3. Temperature Dependence Analysis

The characteristic frequency dependencies of the imaginary part of complex impedance ($Z''(f)$) for P(MMA-*co*-EMA) + 10 wt% of NaI at several different temperature are presented in Figure 4. From the figure, it can be seen that when the temperature increases, the peak of the $Z''(f)$ shifted towards a higher

frequency. All of the other concentration of salts have also been plotted, showing a similar trend. Then, the plot of the relaxation frequency of the bulk conductivity (f_B) that was obtained from the peak of $Z''(f)$ curves in Figure 4 with various temperatures is shown in Figure 5 for different concentrations of salts. Therefore, the relaxation process frequency in the bulk is thermally activated.

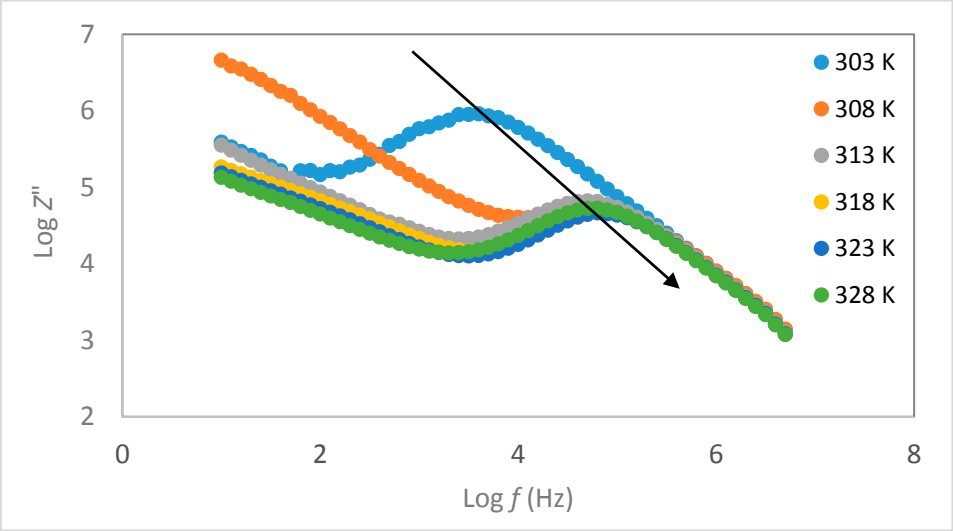

Figure 4. Frequency dependencies of Im(Z) of P(MMA-co-EMA) + 10 wt% NaI at different temperatures.

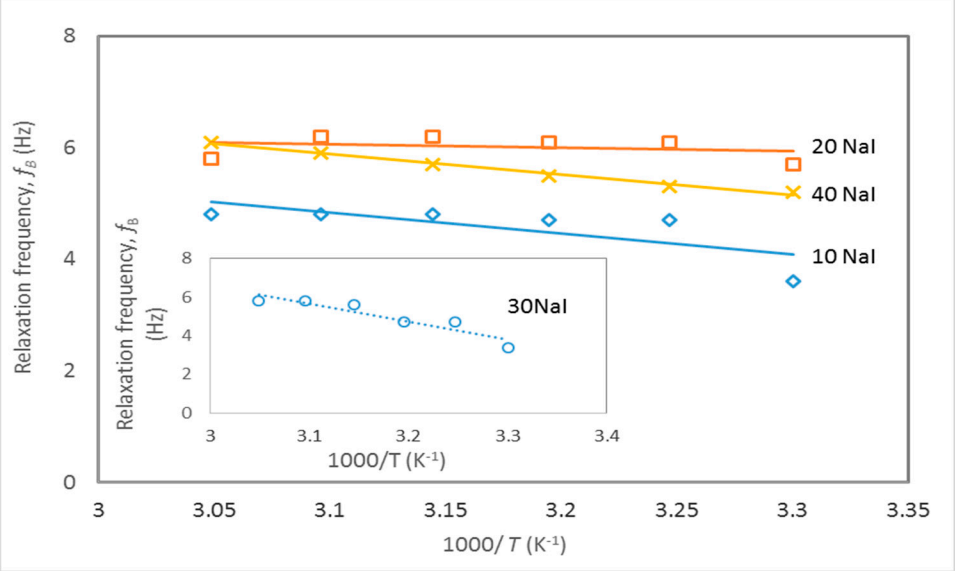

Figure 5. Temperature dependence of the relaxation frequency of the bulk conductivity (f_B) of P(MMA-*co*-EMA) + NaI at different temperatures.

According to Adnan and Mohamed, the activation energy for the relaxation frequency in the bulk, E_f, is in good agreement with that obtained from the Arrhenius plot, and it can be obtained from the temperature dependence of the relaxation frequency of the bulk conductivity, f_B [31]. By using the following Equation (6), the activation energy for the relaxation frequency in the bulk, E_f, can be determined.

$$f_B = f_0 \exp\left(\frac{-E_f}{K(T)}\right) \quad (6)$$

where f_0 is the attempted frequency related to the lattice vibration and k is the Boltzmann constant [32].

The E_f value is the energy required to provide a conductive condition for the migration of ions. The calculated E_f value is presented in Table 1, and from that table, the polymer electrolytes that contain 20 wt% of NaI exhibit the lowest activation energy compared to the others, which is 0.11 eV. It is known that E_f is related to the concentration of the charge carrier and the migration rate of the charge carrier, which is proportional to the ionic conductivity [33]. Therefore, this proves that at this concentration, only a small amount of energy is required to provide the conductive condition for the migration of ions in the polymer electrolytes, hence increasing the ionic conductivity.

Table 1. Activation energy for the relaxation frequency in the bulk, E_f, with various concentrations of NaI.

Concentration of Salt (wt%)	Activation Energy, E_f
10 NaI	0.73
20 NaI	0.11
30 NaI	1.83
40 NaI	0.73

3.4. SEM Studies

Cross-sectional SEM (Scanning Electron Microscope) images of the of P(MMA-*co*-EMA) electrolytes containing 10 wt%, 20 wt%, 30 wt% and 40 wt% of NaI are shown in Figure 6a–d, respectively. The porosity observed in all of the cross-sectional images when NaI was added into the polymer host may be due to the rapid evaporation of THF during the preparation of the film [34,35]. The sizes of the micro-pores are smaller at 20 wt% of NaI (Figure 6b), and this will make the ions move easily in the polymer host and leads to an increase in the ionic conductivity. Meanwhile, with the addition of 30 wt% NaI (Figure 6c), the micro-pores sizes become larger, and it becomes difficult for the ions to move in the polymer electrolyte system. Therefore, this will cause a decrease in the ionic conductivity and gives a higher activation energy compared to the other concentrations of NaI that have been shown earlier. With the further increase of the NaI concentration up to 40 wt% (Figure 6d), the cross-sectional surface becomes rough, and some fractures occur on the surface. Therefore, the broken network will disrupt the pathways of the ions, thus producing lower conductivity in the system.

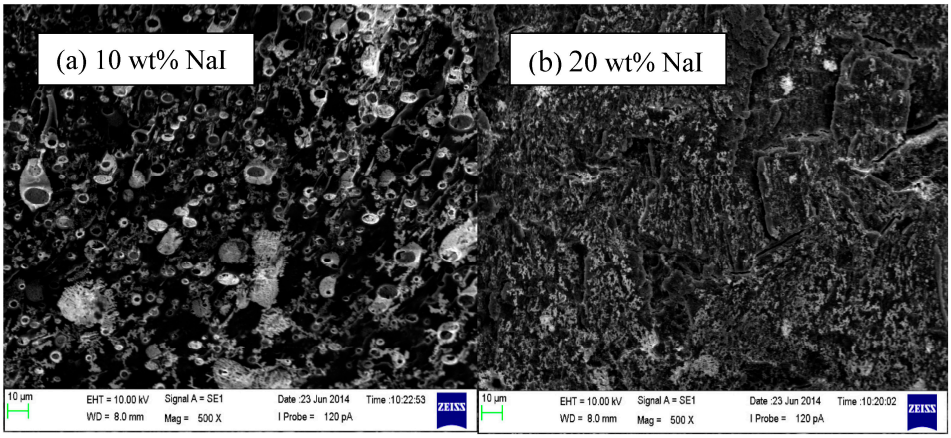

Figure 6. *Cont.*

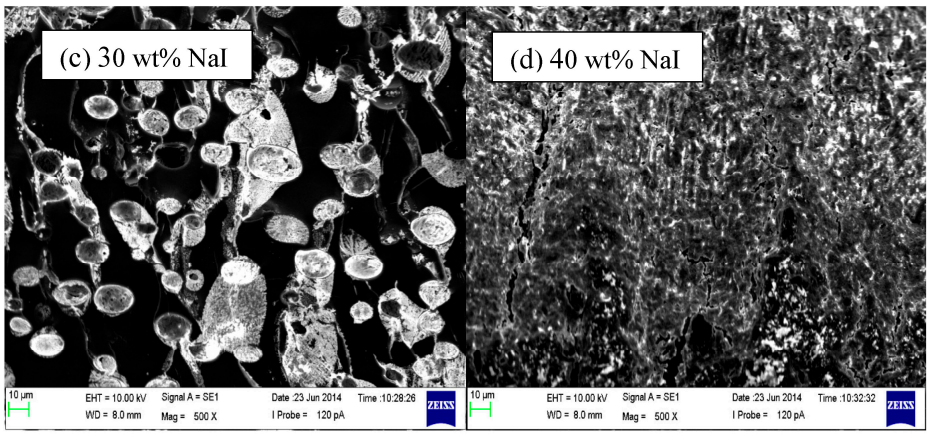

Figure 6. Cross-sectional morphological images of P(MMA-*co*-EMA) + NaI polymer electrolyte films.

3.5. Transference Number

The normalized current *versus* time of 90MMA-*co*-10EMA with the addition of 20 wt% of NaI is plotted in the graph that is shown in Figure 7. From this graph, it is shown that the total ionic transference number is 0.98. This suggests that the charge transport in these polymer electrolyte films is predominantly due to ions [36]. This is consistent with the results from the FTIR analysis and the ionic conductivity study mentioned earlier, which show that both cations (Na^+) and anions (I^-) are fully dissociated and coordinated with the polymer chain, leading to an increase in conductivity.

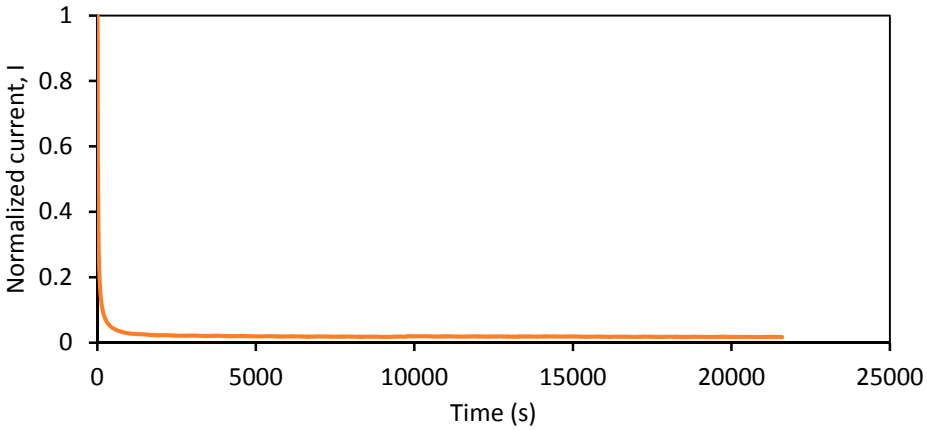

Figure 7. Normalized current *versus* time for polymer electrolyte films with the addition of 20 wt% NaI.

3.6. Linear Sweep Voltammetry

90MMA-*co*-10EMA + 20 wt% NaI was chosen for further analysis to determine the electrochemical stability of the electrolytes using LSV. Figure 8 represents the current-voltage response of the polymer electrolyte film and shows that the decomposition voltage for this film is 2.5 V. This result suggests that the polymer electrolyte is very suitable for applications in DSSC [37].

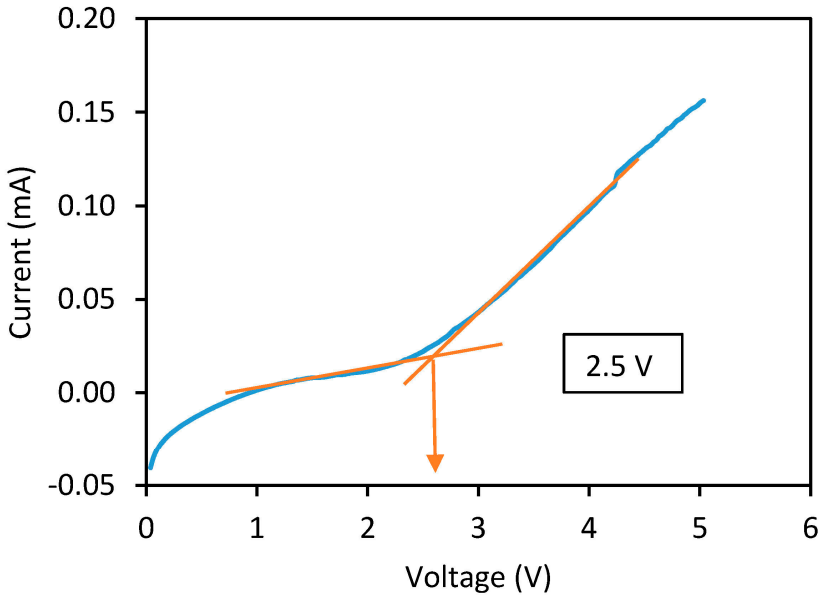

Figure 8. Current *versus* voltage plot of P(MMA-*co*-EMA) with the addition of 20 wt% NaI.

3.7. I–V Measurements

Illustrated in Figure 9 is the photocurrent density-voltage (*J*–V) curve of P(MMA-*co*-EMA) + 20 wt% of NaI-based DSSC under illumination. The mechanism in the DSSC can be explained as follows. As the dye molecules are struck by light, electrons in the dye are injected into the TiO_2 layer. Then, the electrons are collected by the FTO glass electrode and supplied to the external load. The dye molecules are then electrically reduced to their initial states by electrons transferred from the redox coupling (I^-/I_3^-) in the polymer electrolyte. The oxidized ions in the polymer electrolyte diffuse to the Pt electrode to receive electrons [38].

The photovoltaic parameters, such as J_{sc}, V_{oc}, FF and η, were obtained from the intersection of current and voltage from the *J*–V curves under illumination [39]. FTO/TiO_2-dye/P(MMA-*co*-EMA)-NaI-I_2/Pt DSSC shows a photovoltaic response with a J_{sc} of 2.23 mA·cm^{-2}, V_{oc} of 0.76 V, FF of 0.37 and η of 0.62%. Therefore, this proves that the P(MMA-co-EMA) + 20 wt% NaI has the potential to be applied in the DSSC.

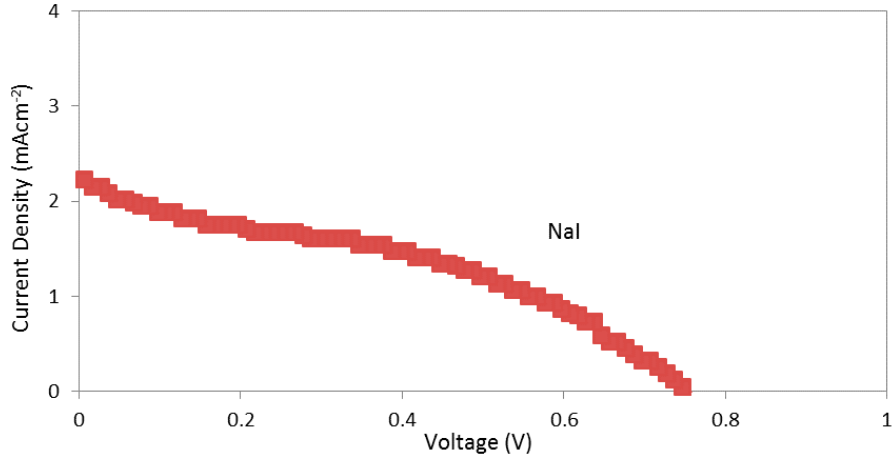

Figure 9. *J–V* curves of the dye-sensitized solar cell assembled with P(MMA-*co*-EMA) + NaI electrolytes.

4. Conclusions

Polymer electrolytes of 90 wt% of MMA and 10 wt% of EMA incorporating different amounts of sodium iodide were successfully prepared using the solution casting method. The shifts of the wavenumber of the carbonyl, ether and methyl groups in the Fourier transform infrared spectra showed that there was an interaction between sodium and iodide ions with the polymer host structure. The electrolyte containing 20 wt% of sodium iodide exhibited the highest ionic conductivity of 5.19×10^{-6} S·cm^{-1} at room temperature and exhibit the highest T_g. From the cross-sectional image, the morphology also shows that the pores are smaller compared to the other concentration, which helps with enhancing the ionic conductivity. The ionic transference number in the polymer electrolytes shows that the charge transport for these electrolytes was predominantly due to the ion. Linear sweep voltammetry data indicated that the copolymer electrolytes were electrochemically stable up to a voltage of 2.5 V. A DSSC has been fabricated using the most conductive electrolyte film and showed an efficiency of 0.62%.

Acknowledgments

The authors would like to extend their gratitude to the University of Malaya for financial support by the Postgraduate Research Fund (PG109/2013A). Nurul Akmaliah Dzulkurnain also thanks the University of Malaya for the Bright Spark University Malaya scholarship awarded to her.

Author Contributions

All listed authors contributed to this work. Nurul Akmaliah Dzulkurnain was responsible for the preparation of the polymer electrolytes films, analyzing the data as well as writing this manuscript; Azizan Ahmad and Nor Sabirin Mohamed propose some constructive explanations and suggestion about the analysis as well as the revisions for this manuscript.

Conflicts of Interest

The authors declare no conflicts of interest.

References

1. O'Regan, B.; Grätzel, M. A low-cost, high-efficiency solar cell based on dye-sensitized colloidal TiO_2 films. *Nature* **1991**, *353*, 737–740.
2. Nogueira, A.F.; de Paoli, M.-A.; Montanari, I.; Monkhouse, R.; Nelson, J.; Durrant, J.R. Electron transfer dynamics in dye sensitized nanocrystalline solar cells using a polymer electrolyte. *J. Phys. Chem. B* **2001**, *105*, 7517–7524.
3. Günes, S.; Sariciftci, N.S. Hybrid solar cells. *Inorg. Chim. Acta* **2008**, *361*, 581–588.
4. Meng, Q.-B.; Takahashi, K.; Zhang, X.-T.; Sutanto, I.; Rao, T.; Sato, O.; Fujishima, A.; Watanabe, H.; Nakamori, T.; Uragami, M. Fabrication of an efficient solid-state dye-sensitized solar cell. *Langmuir* **2003**, *19*, 3572–3574.

5. Hirata, N.; Kroeze, J.E.; Park, T.; Jones, D.; Haque, S.A.; Holmes, A.B.; Durrant, J.R. Interface engineering for solid-state dye-sensitised nanocrystalline solar cells: The use of an organic redox cascade. *Chem. Commun.* **2006**, *14*, 535–537.
6. Yang, Y.; Zhang, J.; Zhou, C.; Wu, S.; Xu, S.; Liu, W.; Han, H.; Chen, B.; Zhao, X.-Z. Effect of lithium iodide addition on poly(ethylene oxide)−poly(vinylidene fluoride) polymer-blend electrolyte for dye-sensitized nanocrystalline solar cell. *J. Phys. Chem. B* **2008**, *112*, 6594–6602.
7. Nishimoto, A.; Watanabe, M.; Ikeda, Y.; Kohjiya, S. High ionic conductivity of new polymer electrolytes based on high molecular weight polyether comb polymers. *Electrochim. Acta* **1998**, *43*, 1177–1184.
8. Ramesh, S.; Arof, A. Ionic conductivity studies of plasticized poly(vinyl chloride) polymer electrolytes. *Mater. Sci. Eng. B Solid* **2001**, *85*, 11–15.
9. Bella, F.; Lamberti, A.; Sacco, A.; Bianco, S.; Chiodoni, A.; Bongiovanni, R. Novel electrode and electrolyte membranes: Towards flexible dye-sensitized solar cell combining vertically aligned TiO2 nanotube array and light-cured polymer network. *J. Membr. Sci.* **2014**, *470*, 125–131.
10. Bella, F.; Ozzello, E.D.; Sacco, A.; Bianco, S.; Bongiovanni, R. Polymer electrolytes for dye-sensitized solar cells prepared by photopolymerization of PEG-based oligomers. *Int. J. Hydrog. Energy* **2014**, *39*, 3036–3045.
11. Bella, F.; Sacco, A.; Salvador, G.P.; Bianco, S.; Tresso, E.; Pirri, C.F.; Bongiovanni, R. First pseudohalogen polymer electrolyte for dye-sensitized solar cells promising for *in situ* photopolymerization. *J. Phys. Chem. C* **2013**, *117*, 20421–20430.
12. Dzulkurnain, N.A.; Hanifah, S.A.; Ahmad, A.; Mohamed, N.S. Characterization of random methacrylate copolymers synthesized using free-radical bulk polymerization method. *Int. J. Electrochem. Sci.* **2015**, *10*, 84–92.
13. Imperiyka, M.; Ahmad, A.; Hanifah, S.A.; Rahman, M.Y.A. Preparation and characterization of polymer electrolyte of glycidyl methacrylate-methyl methacrylate-$LiClO_4$ plasticized with ethylene carbonate. *Int. J. Polym. Sci.* **2014**, *2014*, doi:10.1155/2014/638279.
14. Imperiyka, M.; Ahmad, A.; Hanifah, S.; Rahman, M.Y.A. Role of salt concentration lithium perchlorate on ionic conductivity and structural of (glycidyl methacrylate-*co*-ethyl methacrylate) (70/30) based on a solid polymer electrolyte. *Adv. Mater. Res.* **2013**, *626*, 454–458.
15. Dell, R.M. Batteries—Fifty years of materials development. *Solid State Ion.* **2000**, *134*, 139–158.
16. Ellis, B.L.; Nazar, L.F. Sodium and sodium-ion energy storage batteries. *Curr. Opin. Solid State. Mater.* **2012**, *16*, 168–177.
17. Egashira, M.; Asai, T.; Yoshimoto, N.; Morita, M. Ionic conductivity of ternary electrolyte containing sodium salt and ionic liquid. *Electrochim. Acta* **2011**, *58*, 95–98.
18. Osman, Z.; Isa, K.B.M.; Ahmad, A.; Othman, L. A comparative study of lithium and sodium salts in PAN-based ion conducting polymer electrolytes. *Ionics* **2010**, *16*, 431–435.
19. Bella, F.; Ozzello, E.D.; Bianco, S.; Bongiovanni, R. Photo-polymerization of acrylic/methacrylic gel–polymer electrolyte membranes for dye-sensitized solar cells. *Chem. Eng. J.* **2013**, *225*, 873–879.
20. Su'ait, M.; Ahmad, A.; Hamzah, H.; Rahman, M. Effect of lithium salt concentrations on blended 49% poly(methyl methacrylate) grafted natural rubber and poly(methyl methacrylate) based solid polymer electrolyte. *Electrochim. Acta* **2011**, *57*, 123–131.

21. Ahmad, A.; Rahman, M.; Su'ait, M.; Hamzah, H. Study of MG49-PMMA based solid polymer electrolyte. *Open Mater. Sci. J.* **2011**, *5*, 170–177.
22. Pavia, D.L.; Lampman, G.; Kriz, G.; Engel, R. *Introduction to Organic Laboratory Techniques: A Small Scale Approach*; Saunders College Pub: Philadelphia, PA, USA 1998.
23. De Oliveira, H.; dos Santos, M.; dos Santos, C.; de Melo, C. Electrical properties of PVA/PPY blends. *Synth. Metals* **2003**, *135*, 447–448.
24. Rajendran, S.; Prabhu, M.R.; Rani, M.U. Ionic conduction in poly(vinyl chloride)/poly(ethyl methacrylate)-based polymer blend electrolytes complexed with different lithium salts. *J. Power Sources* **2008**, *180*, 880–883.
25. Kumar, D.; Hashmi, S. Ion transport and ion-filler-polymer interaction in poly(methyl methacrylate)-based, sodium ion conducting, gel polymer electrolytes dispersed with silica nanoparticles. *J. Power Sources* **2010**, *195*, 5101–5108.
26. Wu, S. Phase structure and adhesion in polymer blends: A criterion for rubber toughening. *Polymer* **1985**, *26*, 1855–1863.
27. Nagaoka, K.; Naruse, H.; Shinohara, I.; Watanabe, M. High ionic conductivity in poly(dimethyl siloxane-*co*-ethylene oxide) dissolving lithium perchlorate. *J. Polym. Sci. Polym. Lett. Ed.* **1984**, *22*, 659–663.
28. Kobayashi, N.; Uchiyama, M.; Shigehara, K.; Tsuchida, E. Ionically high conductive solid electrolytes composed of graft copolymer-lithium salt hybrids. *J. Phys. Chem.* **1985**, *89*, 987–991.
29. Subban, R.H.Y. Some Properties of plasticized and Composite PVC-Based Polymer Electrolytes and LiCoO2/PVC-LiCF3SO3-SiO2/MCMB Electrochemical Cells. Ph.D. Thesis, University of Malaya, Kuala Lumpur, Malaysis, 2004.
30. Johansson, A.; Gogoll, A.; Tegenfeldt, J. Diffusion and ionic conductivity in $Li(CF_3SO_3)$ PEG_{10} and $LiN(CF_3SO_2)_2$ PEG_{10}. *Polymer* **1996**, *37*, 1387–1393.
31. Adnan, S.; Mohamed, N. Electrical properties of novel $Li_{4.08}Zn_{0.04}Si_{0.96}O_4$ ceramic electrolyte at high temperatures. *Ionics* **2014**, *20*, 1641–1650.
32. Orliukas, A.; Kezionis, A.; Kazakevicius, E. Impedance spectroscopy of solid electrolytes in the radio frequency range. *Solid State Ion.* **2005**, *176*, 2037–2043.
33. Buraidah, M.; Teo, L.; Majid, S.; Arof, A. Ionic conductivity by correlated barrier hopping in NH_4I doped chitosan solid electrolyte. *Phys. B* **2009**, *404*, 1373–1379.
34. Su'ait, M.; Ahmad, A.; Hamzah, H.; Rahman, M. Preparation and characterization of PMMA–MG49–LiClO4 solid polymeric electrolyte. *J. Phys. D Appl. Phys.* **2009**, *42*, doi:10.1088/0022-3727/42/5/055410.
35. Rajendran, S.; Sivakumar, P.; Babu, R.S. Studies on the salt concentration of a PVdF–PVC based polymer blend electrolyte. *J. Power Sources* **2007**, *164*, 815–821.
36. Subba Reddy, C.V.; Sharma, A.; Narasimha Rao, V. Conductivity and discharge characteristics of polyblend (PVP+ PVA+ KIO_3) electrolyte. *J. Power Sources* **2003**, *114*, 338–345.
37. Rani, M.S.A.; Rudhziah, S.; Ahmad, A.; Mohamed, N.S. Biopolymer electrolyte based on derivatives of cellulose from kenaf bast fiber. *Polymers* **2014**, *6*, 2371–2385.
38. Ichino, T.; Takeshima, Y.; Takeshima, M.; Nishi, S. *Japanese Patent Publication*; NTT Co.: Tokyo, Japan, 1995; p. 335258.

39. Rahman, M.; Salleh, M.; Talib, I.; Yahaya, M. Light intensity and temperature dependence on performance of a photoelectrochemical cells of ITO/TiO_2/PVC–$LiClO_4$/graphite. *Ionics* **2007**, *13*, 241–244.